Physicochemical Investigation of Lightfast AgCl and AgBr Nanoparticles Synthesized by a Novel Solid−Solid Reaction

Pietro Calandra,[†] Alessandro Longo,[‡] Vito Marcianò,[§] and Vincenzo Turco Liveri*,[†]

Dipartimento di Chimica-Fisica, Università degli Studi di Palermo, Viale delle Scienze Parco d'Orleans II, 90128 Palermo, Italy, ISMN, Istituto per lo Studio dei Materiali Nanostrutturati, Via Ugo La Malfa 153, 90146 Palermo, Italy, and Dipartimento di Medicina Sperimentale, Università di Palermo, Policlinico Universitario "P. Giaccone", 90128 Palermo, Italy

Received: November 13, 2002; In Final Form: May 15, 2003

Small size AgX (X = Br, Cl) nanoparticles have been synthesized by a novel solid−solid reaction performed by mixing two dry dispersions of $AgNO_3$ and KX nanoparticles in AOT/*n*-heptane solutions. UV−vis investigation ascertained that formation of nanosized particles taking place after the mixing process is fast and complete. Microcalorimetric measurements of the thermal effect coupled with the mixing process suggest the occurrence of confinement effects and adsorption of the surfactant molecules at the nanoparticle surface, hinting at formation of charged nonstoichiometric surfactant-coated nanoparticles. The analysis of SAXS spectra shows that salt-containing AOT reversed micelles are slightly bigger and more polydisperse than bare AOT ones. After the mixing process, from all liquid samples, interesting AgX/AOT composites at high AgX nanoparticle concentration can be prepared by simple evaporation of the organic solvent. Size, polydispersity, and crystal structure of AgX nanoparticles embedded in AOT matrix were determined by WAXS and TEM.

Introduction

Synthesis and physicochemical characterization of silver halide nanoparticles have been drawing researchers' and engineers' attention for decades because of their peculiar properties. First of all, these substances are semiconductors and their nanosized crystals show marked quantum size effects, so much so that AgI was one of the first materials in which excitonic quantum confinement effects were observed.[1] Another interesting property of silver halides is their high ionic conductivity, due mainly to the mobile silver ions that can easily hop from one Frenkel defect to another[2] and that has been found to be greatly enhanced by the dispersion of a second phase in the ionic conductive matrix or by the heterogeneous mixture with other solid ionic conductors.[3] If nanosized crystals are used as dispersed phase, due to critical size-dependent changes in the nanoparticle free energy, interesting variations in the ionic conductivity performances can be expected.

However, the most known peculiarity of silver halides is probably their behavior under exposure to light, which is at the basis of their use as source materials in photographic processes. The photogenerated electron−hole pair is able to reduce an interstitial mobile Ag^+ ion, thus forming a silver atom. If repeated absorption of photons occurs, a cluster of silver atoms can ultimately be formed in a process usually called latent image formation. Since this process is strongly influenced by the crystal structure, researchers' efforts have been directed to control crystal size and shape in order to increase the photographic resolution, light sensitivity, and chemical stability. Moreover, through the absorption of suitable organic molecules at the silver halide crystal surface, it is possible to widen the sensitivity range to the whole visible spectrum, thus increasing both black-and-white and color photography performances.[4−7]

On the other hand, if suitable conditions to avoid photodecomposition are found, silver halide nanoparticles can also have important applications in heterogeneous catalysis. Calzaferri et al. in 1996[8] found that, under UV irradiation, AgCl supported on SnO_2 in the presence of a small excess of Ag^+ and dispersed in aqueous solution is able to catalyze photooxidation of water. Afterward, Kakuta et al.,[9] using AgBr supported on silica showed that it is a good catalyst for hydrogen generation from CH_3OH/H_2O solutions. More recently, Yamashita et al.[10] reported on the catalytic activity of AgCl for the photoconversion of NO.

Taking into account the enhanced properties of small nanoparticles, with the present contribution we exploit the recently proposed synthetic route based on the solid−solid reaction in liquid phase of AOT reversed micellar solutions to synthesize small and lightfast AgX (X = Br, Cl) nanoparticles.[11,12] In particular, the dry synthetic method reported here is a solid-state reaction performed by mixing two water-free dispersions of $AgNO_3$ and KX nanoparticles in AOT/*n*-heptane solutions.

Experimental Part

Materials. Sodium bis(2-ethylhexyl)sulfosuccinate (aerosol-OT, AOT Sigma 98%) was stored in a desiccator and used after at least one week. *n*-Heptane (Aldrich 99% spectrophotometric grade), silver nitrate (Carlo Erba ≥ 99.8%, ACS. reagent), potassium chloride (Carlo Erba ≥ 99.5% R.P. reagent), and Potassium Bromide (Aldrich ≥ 99.8%, ACS Reagent) were used as received. Bidistilled water was used in all experiments.

* Corresponding author. E-mail turco@unipa.it.
[†] Università degli Studi di Palermo.
[‡] Istituto per lo Studio dei Materiali Nanostrutturati.
[§] Università di Palermo, Policlinico Universitario "P. Giaccone".

10.1021/jp027455q CCC: $25.00
Published on Web 06/24/2003

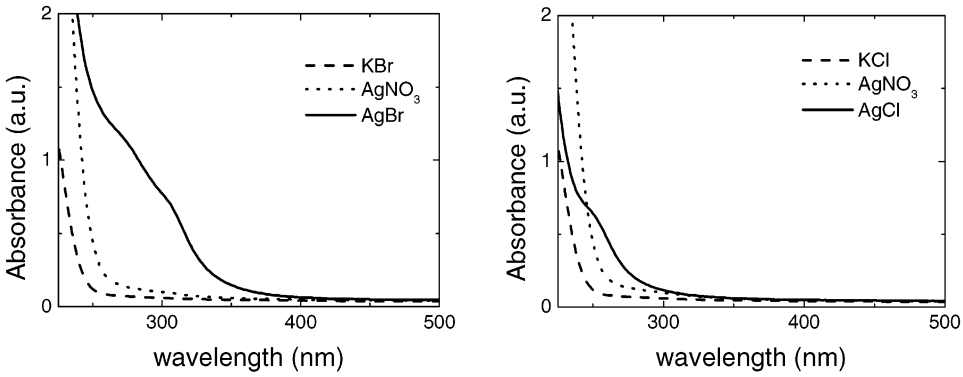

Figure 1. Typical UV−vis spectra of salt-containing AOT/*n*-heptane solutions at [AOT] = 5×10^{-2} mol kg^{-1}, [salt] = 3×10^{-3} mol kg^{-1} (AgX spectra refer to systems at $R = 2$).

Methods

The procedure followed for the preparation of dry AOT/*n*-heptane solutions containing $AgNO_3$ and KX (X = Br, Cl) consists of three steps: first, salt-containing w/o microemulsions were prepared by adding the appropriate amount of water/AOT/*n*-heptane microemulsion ([water]/[AOT] = 8) to a weighed quantity of salt. Then, by keeping these w/o microemulsions in a desiccator connected to a diaphragm vacuum pump (MZ2C, Vacuubrand), the corresponding salt−surfactant composites were obtained. Finally, the salt−surfactant composites were dissolved in the appropriate amount of pure *n*-heptane to give the original AOT concentration. Further details on this preparation procedure have been previously reported.[11,12]

The solid−solid reaction

$$AgNO_3 + KX \rightarrow AgX + KNO_3 \qquad (1)$$

in a confined space was performed at 25 °C by mixing two dry dispersions of $AgNO_3$ and KX in AOT/*n*-heptane solutions. The amounts of these solutions were chosen in order to obtain the desired $AgNO_3$-to-KX molar ratio (R). In these solutions, AOT and salt concentrations were fixed at 5×10^{-2} and 3×10^{-3} mol kg^{-1}, respectively. Even if the reaction leads to the formation of two species (AgX and KNO_3), hereafter, for simplicity, the mix will be identified by the silver halide salt synthesized (AgBr or AgCl).

All measurements were carried out using freshly prepared liquid samples, because preliminary experiments showed the occurrence of aging effects attributable to a slow nanoparticle growth occurring after their synthesis. This nanoparticle growth process can be attributed to the intermicellar material exchange occurring as a consequence of micellar encounters and coalescence.

UV−vis measurements were carried out recording UV−vis spectra in the wavelength range of 220−500 nm by a Perkin-Elmer Lambda 900 spectrometer using an AOT/*n*-heptane solution at the same surfactant concentration as blank. A NIR spectrum was also recorded for each sample in the 1800−2200 nm range to check the amount of residual water, which was found to be always less than 0.3 molecules for each AOT molecule.[13]

SAXS patterns have been recorded by a laboratory instrumentation consisting of a Philips PW 1830 X-ray generator providing Cu Kα, Ni filtered ($\lambda = 1.5418$ Å) radiation with a Kratky small-angle camera in the "finite slit height" geometry equipped with a step scanning motor and scintillation counter. Each scattering spectrum was subtracted by the cell and solvent contributions. Best-fit analyses were performed by the CERN minimization program called MINUITS. For AgBr/AOT/*n*-heptane system, SAXS as well as UV−vis spectra at $R = 1$ were not recorded because this sample becomes quickly opalescent.

Calorimetric measurements were carried out at 25 °C with a thermal activity monitor (LKB) equipped with a flow-mix cylinder (LKB 2277−204). As a standard procedure, two dry dispersions of $AgNO_3$ and KX in AOT/*n*-heptane solutions, both at [AOT] = 5×10^{-2} mol kg^{-1} and [salt] = 3×10^{-3} mol kg^{-1} were driven by two peristaltic pumps (Gilson, Minipulse 2) into the calorimetric cell where the reaction took place and the flow rates were determined by weight. The desired R value was obtained by suitably varying the flow rate ratio (ϕ_1/ϕ_2) of the two peristaltic pumps. Moreover, the total flow rate ($\phi_1 + \phi_2$) was chosen in order to ensure in all cases the occurrence of the totality of the thermal effect inside the calorimeter chamber ($\phi_1 + \phi_2 \leq 10^{-2}$ g s^{-1}). The baseline was determined by mixing two AOT/*n*-heptane solutions at [AOT] = 5×10^{-2} mol kg^{-1}. Preliminary experiments showed that the thermal effect due to dilution of AOT/*n*-heptane systems containing KX or $AgNO_3$ is negligible. The experimental molar enthalpy (ΔH) of the AgX formation was calculated using the equation:

$$\Delta H = q/([\text{salt}]^*\phi_{\text{def}}) \qquad (2)$$

where q is the calorimetric signal and ϕ_{def} is the flow rate of the solution containing the reagent in defect.

AgX/AOT composites were prepared by keeping the dispersions of AgX in AOT/*n*-heptane solutions in a desiccator connected to a diaphragm vacuum pump (MZ2C, Vacuubrand).

WAXS diffractograms of AgX/AOT composites were recorded with a Philips diffractometer (PW1050/39 X change) equipped with a copper anode providing a Ni-filtered Cu Kα 1.5418 Å radiation.

Transmission electron microscopy (TEM) images were obtained with a JEOL 1220 T transmission electron microscope operating at 120 kV representing a suitable acceleration voltage to obtain good resolution with little radiation damage of the material. The samples for TEM were prepared by placing a drop of AgX-containing AOT/*n*-heptane solution onto a carbon−copper grid and allowing the evaporation of the solvent at room temperature.

Results and Discussion

Typical UV−vis spectra of dispersions of AgX in AOT/*n*-heptane solutions at [AOT] = 5×10^{-2} mol kg^{-1}, [salt] = 3×10^{-3} mol kg^{-1} and $R = 2$ recorded immediately after the mixing process are shown in Figure 1 where those of the reacting solutions are also reported as references. The figure clearly shows that in the mix spectra new absorption bands are present.

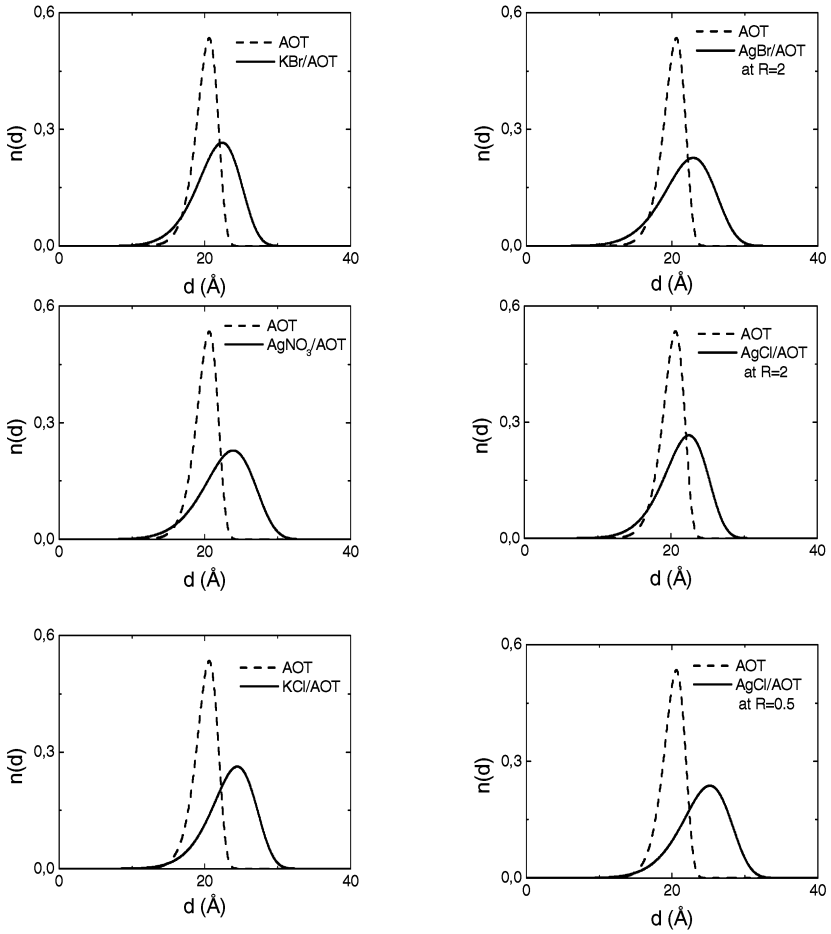

Figure 2. Comparison between the micellar core diameter (d) distribution functions $n(d)$ of AOT/*n*-heptane solution ([AOT] = 5×10^{-2} mol kg^{-1}, dashed line) and some representative salt-containing AOT/*n*-heptane solutions ([salt] = 3×10^{-3} mol kg^{-1} and [AOT] = 5×10^{-2} mol kg^{-1}, continuous line).

These bands, ascribable to the presence of AgX,[14] were found to be well developed immediately after the mixing process, thus revealing that the solid−solid reaction leading to the AgX formation is rapid and complete. For both salts, no significant change in band shape and position as a function of R ($0.5 \leq R \leq 2$) was observed. Taking into account the correlation between nanoparticle diameter and band position,[14−17] this finding indicates that AgX nanoparticle size is only slightly influenced by the R value. This indicates that the concentration of reversed micelles is sufficiently high to be the factor determining the particle size.

As regards the spectrum of AgBr, it is worth noting that the UV absorption band is constituted by:

(i) a first broad absorption centered at about 300 nm due to the direct exciton absorption. Its position, corresponding to an energy gap of about 4.2 eV is blue-shifted with respect to that of bulk AgBr (2.7 eV, 475 nm). This behavior is a well-known quantum size effect affecting semiconductor nanoparticles and is itself an evidence that AgBr is nanosized.

(ii) a second and more intense broad absorption at shorter wavelength (about 270 nm) due to the spin−orbit interaction splitting of the direct exciton absorption.[14,15] The splitting energy can only roughly be estimated because these absorptions are not well resolved and results to be of about 0.5 eV in agreement with literature value.[15] Since experimental and theoretical investigations[14−16] showed that $(AgBr)_n$ with $n \leq 4$ do not show split excitonic bands, the peculiar absorption feature in Figure 1 suggests that nanoparticles are composed by at least four AgBr molecular units.

Concerning the spectra of dispersions of AgCl in AOT/*n*-heptane solutions, the direct exciton absorption bands are less intense than those of AgBr. They are centered at about 250 nm corresponding to an energy gap value of 5.1 eV that, compared with the bulk AgCl value of 3.2 eV, reveals that also this material is nanosized. Moreover, the UV spectra do not show spin−orbit interaction splitting, probably due to the fact that the excitonic absorption occurs in a wavelength region ($\lambda <$ 220 nm) hardly accessible by our instrumentation. Incidentally, it is important to note that no optical absorption has been observed in the 300−500 nm range, where Ag metal has been reported to absorb,[15,18] even at long times and under sunlight exposure, thus excluding silver formation and pointing out the lightfastness of these systems. This surprising feature can be probably ascribed to the adsorption of the surfactant molecules at the nanoparticle surface. In fact, the adsorbed surfactant could act as an electron−hole scavenger and/or could offer a favored pathway for their recombination, thus avoiding electron−silver ion reaction.

Information on the size of $AgNO_3$, KX, and AgX nanoparticles confined in the core of AOT reversed micelles were achieved by SAXS measurements on salt-containing AOT/*n*-heptane solutions. All SAXS spectra were found to be well described by a model of noninteracting homogeneous scattering spheres with a size distribution described by the function $n(d)$ where d is the sphere diameter. Since X-ray scattering signal originates from the contrast between adjacent regions with different electron densities, taking into account the peculiar structure of salt-containing AOT reversed micelles,[19,20] the

TABLE 1: Mean Diameter (d) and b Values of the Core of Salt-Containing AOT Reversed Micelles[a]

	R	d_m(Å)	b
AOT		20.8	18
KBr		21.4	8
$AgNO_3$		22.8	8
KCl		23.4	9
AgBr	0.5	20.8	4
AgBr[a]	1		
AgBr	2	22.2	7
AgCl	0.5	24.4	10
AgCl	1	25.6	17
AgCl	2	21.4	8

[a] Opalescent sample.

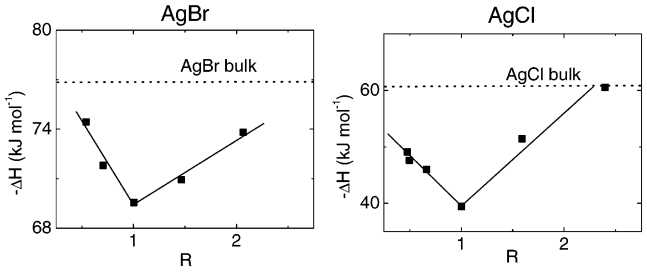

Figure 3. Experimental molar enthalpies (ΔH) as a function of the ratio R at [AOT] = 5×10^{-2} mol kg^{-1} and [salt] = 3×10^{-3} mol kg^{-1}.

scattering spheres of the model are to be interpreted as the bare or salt-containing micellar cores. The fitting procedure, whose details have been previously reported,[11] allows the determination of the micellar core mean diameter (d_m) and the parameter b that, governing the shape of the size distribution function, is a quantitative descriptor of the size polydispersity. The derived parameters are summarized in Table 1, and the size distribution functions $n(d)$ are shown in Figure 2. A perusal of Table 1 and Figure 2, indicates that salt-containing cores of AOT reversed micelles are bigger and more polydisperse than the bare AOT ones. Moreover, a comparison of the fitting parameters d_m and $n(d)$ distribution functions of all salt-containing systems shows that micellar size and polydispersity are only slightly influenced by the nature of the salt entrapped in reversed micelles and the R value.

It must be pointed out that although SAXS data do not allow the direct determination of the nanoparticle size, a comparison between the $n(d)$ functions for the bare AOT/n-heptane solutions and the salt-containing ones leads us to conclude that AgX nanoparticle size must be very small and that their formation takes place via redistribution of the two reacting salts ($AgNO_3$ and KX) among the reversed micelles.

A specific advantage of the present method is that nanoparticles are smaller than those synthesized by the classical way, i.e., by mixing two water/AOT/n-heptane microemulsions[21−23] containing, in the water pool, silver nitrate and alkaline halide salts, respectively (diameter 2−40 nm). This can be determined by the high salt concentration and the absence of water. As regards the former effect, it has been shown[21] that for intermicellar nucleation to occur, the number of ions inside the micelle must be greater than the critical nucleation number. In dry reversed micelles, the very high salt-to-AOT molar ratio makes the micellar ion occupancy very high, causing the formation of a high number of nuclei. On the other hand, the absence of water makes micellar cores more rigid, thus leading to a lower rate of intermicellar exchange of material and to a less efficient nanoparticle growth. As a consequence of both effects, the formation of several nuclei, followed by an exiguous growth, gives small nanoparticles. Another advantage of this method is that, AgX concentration and AgX-to-AOT molar ratio are about five times higher than those typically reached by means of w/o microemulsions,[21,22] thus making these systems more attractive for technological applications.

Further information on AgX nanoparticles were obtained by microcalorimetry. The experimental molar enthalpies (ΔH) of reaction 1 occurring in the core of dry AOT reversed micelles, are reported in Figure 3 as a function of R. The departure of the experimental ΔH values from the molar enthalpies of the same processes in bulk state (−76.82 and −60.56 kJ mol^{-1} for AgBr and AgCl, respectively)[24] can be at least qualitatively rationalized in terms of confinement effects due to surfactant adsorption at the nanoparticle surface and to the presence of small-size particles with a high fraction of surface atoms. Moreover, the V-shaped trends suggest formation at $R \neq 1$ of charged, enthalpically more stable, nonstoichiometric nanoparticles. The lower enthalpic stability of systems synthesized in stoichiometric condition is probably the reason AOT/n-heptane solution containing AgBr at $R = 1$ becomes quickly opalescent. It must be stressed that, to the best of our knowledge, experimental data on the energetics of solid−solid reactions in

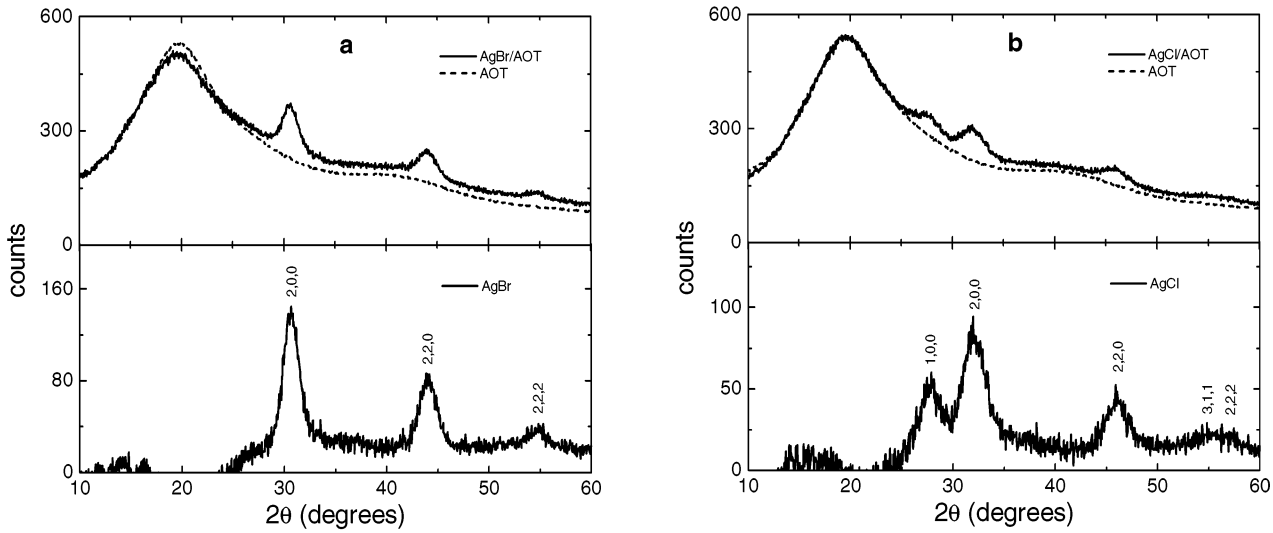

Figure 4. Comparison between WAXS spectra of pure AOT and (a) AgBr/AOT, (b) AgCl/AOT composites at $R = 2$ recorded immediately after their preparation. The lower panels show the difference spectra on which the Debye-Sherrer analyses were carried out.

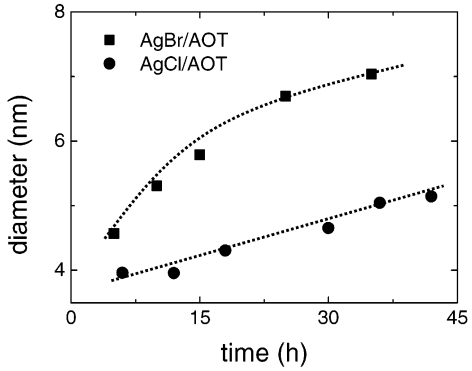

Figure 5. Time dependence of the AgX nanocrystallite diameter at $R = 2$ derived by the Debye-Sherrer analysis.

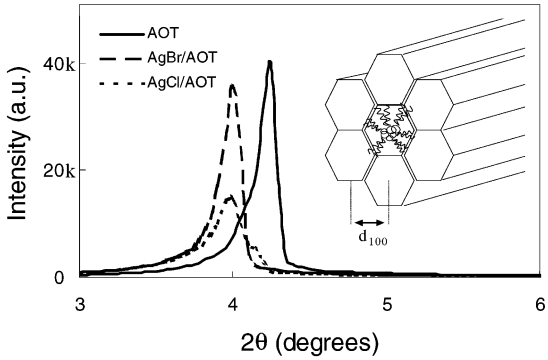

Figure 6. WAXS spectra of pure AOT and AgX/AOT composites at $R = 2$ recorded immediately after their preparation.

microheterogeneous systems are absent in the literature, so these data could represent a test stand for theoretical calculations.

It is worth noting that this novel way of nanoparticle synthesis offers some advantages with respect to the mechano-synthesis performed by the milling of solids. In fact, it is well-known that the latter synthetic route is not useful for obtaining nanoparticles smaller than 10 nm.[25,26] Moreover, solid-state reaction occurring in mechano-synthesis is generally not quantitative, since the reaction involves only interfacial atoms and the diffusion of chemical species is negligible in the solid state. On the contrary, the method presented here, using very small particles characterized by a high reactive surface and dispersed in a liquid medium, bypasses these drawbacks and offers the further advantage of giving, in appropriate conditions, nanosized products thanks to the confinement in the core of AOT reversed micelles.

In view of their potential technological applications, by fast evaporation under vacuum of the organic solvent of dispersions of AgX in AOT/*n*-heptane solutions, AgX/AOT composites were prepared. Typical WAXS spectra of freshly prepared composites at $R = 2$ are reported in Figure 4 where the spectrum of pure AOT is also shown as reference. Superimposed to the AOT background, it can be noted the presence of the diffraction peaks due to AgX nanocrystals, which unequivocally indicates their occurrence in AgX/AOT composites. Peak analysis also showed that the structure of both silver halides nanoparticle is the fcc chlorargyrite structure.[3,9] No significant intensity anomalies were observed, and this suggests a random orientation of grains. Moreover, the absence of peak at about 38 degrees, where metal silver is reported to diffract,[9] excludes the presence of silver crystals in composites. It is worth noting that no peak attributable to KX was found showing that this material is amorphous and/or finely dispersed in the AOT matrix.

Debye-Sherrer analysis of peak widths gave a rough estimation of nanoparticle size of 4.5 and 4.0 nm for AgBr and AgCl, respectively. To test the stability of AgX nanoparticles in these composites, WAXS measurements were carried out as a function of time. The only feature observed was a slow peak width reduction pointing out a nanoparticle growth. Figure 5 shows the time dependence of the nanocrystallite diameters derived through the Debye-Sherrer analysis.

This behavior can be rationalized considering the particular mobility of the silver ion that could drive a slow structural rearrangement of nanoparticles leading to bigger crystalline domains. It can be seen that this process occurs more slowly in AgCl/AOT composites than in AgBr/AOT ones.

Additional structural information can be achieved by inspection of the low-angle part of the WAXS diffractograms. Figure

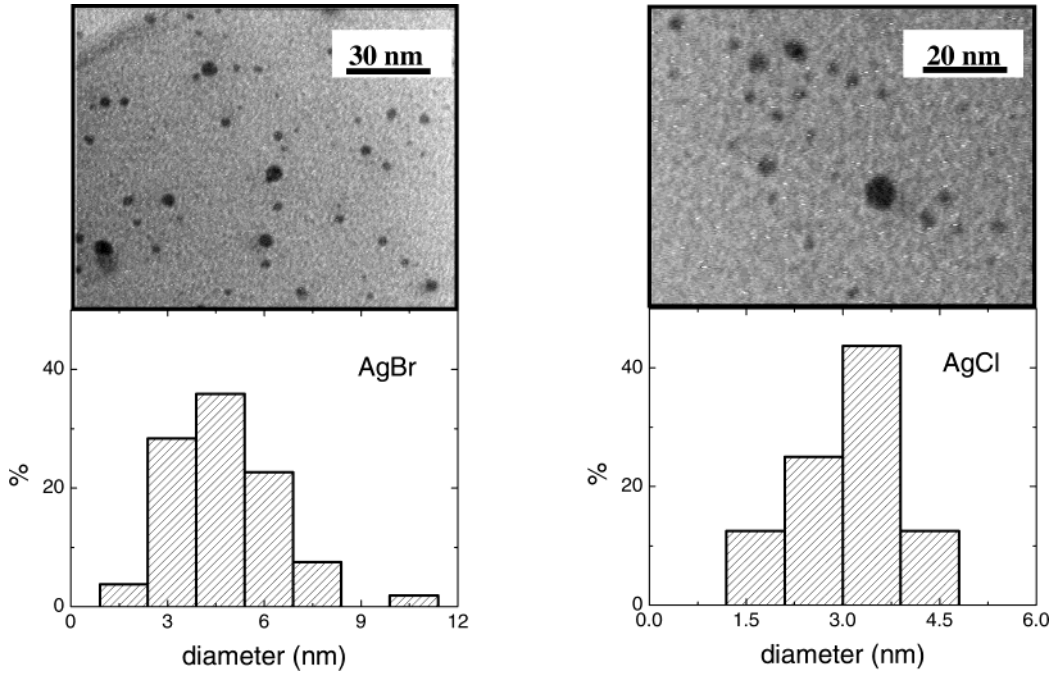

Figure 7. Typical micrographs and statistical analyses of AgBr/AOT (left) and AgCl/AOT (right) composites at $R = 2$.

TABLE 2: WAXS Peak Positions and Corresponding d_{100} Values for Pure AOT and AgX/AOT Composites

sample	2θ (degrees)	d_{100} (Å)
AOT	4.00	20.8
AgBr/AOT	4.25	22.1
AgCl/AOT	4.25	22.1

6 reports the diffractograms in the range 3−6 degrees. In this region the observed peak is due to the typical two-dimensional hexagonal structure of solid AOT and in particular it corresponds to the lattice parameter d_{100}[27] (see insert in Figure 6). The peak positions and the corresponding d_{100} values of the pure AOT and AgX/AOT composites are reported in Table 2. The slightly higher d_{100} value in AgX/AOT composites with respect to the pure AOT can be ascribed to the fine dispersion of KNO_3 in amorphous state inside the core of AOT rods, whereas the lower peak intensity in AgX/AOT composites indicates a structural disorder due to the presence of randomly dispersed AgX nanoparticles.

Nanoparticle size was evaluated also by transmission electron microscopy (TEM). Two typical micrographs, referring to AgBr/AOT and AgCl/AOT composites ($R = 2$), respectively, taken 1 h after their preparation are shown in Figure 7 together with the statistical analyses. For each sample, the size distribution was generated examining about 150 nanoparticles.

It can be noted that AgX nanoparticles are nearly spherical with an average diameter of 4.5 and 3.0 nm for AgBr and AgCl, respectively. For AgCl/AOT composites, no substantial difference either in nanoparticle average size or polydispersity was found as a function of *R*. Apart from rare small aggregates of nanoparticles, in all samples only isolated and randomly distributed nanoparticles are present, showing the absence of nanoparticle−nanoparticle interactions.

It is worth noting that nanoparticle size in composites is significantly greater than that found in liquid samples. This difference can be ascribed to ripening/agglomeration effects triggered by the progressive increase of nanoparticle concentration occurring during composite preparation.

Conclusions

This study showed that simple mixing of two dry dispersions of $AgNO_3$ and KX (X = Br, Cl) nanoparticles in AOT/*n*-heptane solutions, is a good technique to synthesize very small and lightfast AgX nanoparticles via solid−solid reaction in the liquid phase at room temperature. The AgX nanoparticle formation occurs rapidly and quantitatively through re-distribution of the $AgNO_3$ and KX salts among the dry AOT reversed micelles leading to AOT/*n*-heptane solutions containing AgX nanoparticles at relatively high concentration. Confinement effects, attributed to surfactant adsorption and nanoparticle quantum size effects have been detected.

By evaporation of the organic solvent, it is possible to prepare interesting AgX/AOT composites, containing, as assured by WAXS and TEM data analysis, quite monodisperse, noninteracting nearly spherical and crystalline AgX nanoparticles. Nanoparticle size in composites is significantly greater than that found in liquid samples and it slightly increases with time.

Acknowledgment. Financial support from MIUR 60% is gratefully acknowledged.

References and Notes

(1) Vogelsang, H.; Husberg, O.; von der Osten, W. *J. Lumin.* **2000**, *86*, 87−94, and references therein.
(2) Funke, K.; Wilmer, D.; Lauxtermann, T.; Holzgreve, R.; Bennington, S. M. *Solid State Ionics* **1996**, *86*−*88*, 141−146.
(3) Rogez, J.; Garnier, A.; Knauth, P. *J. Phys. Chem. Solids* **2002**, *63*, 9−14, and references therein.
(4) Van Renterghem, W.; Goessens, C.; Schryvers, D.; Van Landuyt, J.; Verrept, P.; Bollen, D.; Van Roost, C.; De Keyzer, R. *J. Cryst. Growth* **1998**, *187*, 410−420.
(5) Rubtsov, I. V.; Ebina, K.; Satou, F.; Oh, Ji-Won; Kumazaki, S.; Suzumoto, T.; Tani, T.; Yoshihara, K. *J. Phys. Chem. A* **2002**, *106*, 2795−2802.
(6) Marchetti, A. P.; Muenter, A. A.; Baetzold, R. C.; McCleary, R. T. *J. Phys. Chem. B* **1998**, *102*, 5287−5297.
(7) Araki, T.; Ito, E.; Oichi, K.; Mitsumoto, R.; Sei, M.; Oji, H.; Yamamoto, Y.; Ouchi, Y.; Seki, K.; Tarata, Y.; Edamatsu, K.; Yokoyama, T.; Ohta, T.; Kitajima, Y.; Watanabe, S.; Yamashita, K.; Tani, T. *J. Phys. Chem. B* **1997**, *101*, 10378−10385.
(8) Pfanner, K.; Gfeller, N.; Calzaferri, G. *J. Photochem. Photobiol. A: Chem.* **1996**, *95*, 175−180.
(9) Kakuta, N.; Goto, N.; Ohkita, H.; Mizushima, T. *J. Phys. Chem. B* **1999**, *103* (29), 5917−5919.
(10) Yamashita, Y.; Aoyama, N.; Takezawa, N.; Yoshida, K. *Environ. Sci. Technol.* **2000**, *34* (24), 5211−5214.
(11) Calandra, P.; Longo, A.; Turco Liveri, V. *Colloid Polym. Sci.* **2001**, *279*, 1112−1117.
(12) Calandra, P.; Longo, A.; Turco Liveri, *J. Phys. Chem. B* **2003**, *107*, 25−30.
(13) Giordano, C.; Longo, A.; Turco Liveri, V.; Venezia, A. M. *Colloid Polym. Sci.* **2003**, *281*, 229−238.
(14) Correa, N. M.; Zhang, H.; Schelly, Z. A. *J. Am. Chem. Soc.* **2000**, *122*, 6432−6434.
(15) Zhang, H.; Mostafavi, M. *J. Phys. Chem. B* **1997**, *101*, 8443−8448.
(16) Zhang, H.; Schelly, Z. A.; Marynick, D. S. *J. Phys. Chem. A* **2000**, *104*, 6287−6294.
(17) Glaus, S.; Calzaferri, G. *J. Phys. Chem.* **1999**, *103*, 5622−5630.
(18) Petit, C.; Lixon, P.; Pileni, M. P. *J. Phys. Chem.* **1993**, *97*, 12974−12983.
(19) North, A. N.; Dore, J. C.; McDonald, J. A.; Robinson, B. H.; Heenan, R. K.; Howe, A. M. *Colloids Surf.* **1986**, *19*, 21−29.
(20) Mackeben, S.; Müller-Goymann, C. C. *Int. J. Pharm.* **2000**, *196*, 207−210.
(21) Bagwe, R. P.; Khilar, K. C. *Langmuir* **1997**, *13*, 6432−6438.
(22) D'Aprano, A.; Pinio, F.; Turco Liveri, V. *J. Solution Chem.* **1991**, *20* (3), 301−306.
(23) Johansson, K. P.; Marchetti, A. P.; McLendon, G. L. *J. Phys. Chem.* **1992**, *96*, 2873−2879.
(24) *Handbook of Chemistry and Physics*, 67th ed.; CRC Press Inc.: Boca Raton, FL, 1986−1987.
(25) Goya, G. F.; Rechenberg, H. R. *J Magn. Magn. Mater.* **1999**, *196*, 191−192.
(26) Millot, N.; Begin Colin, S.; Perriat, P.; Le Caër, G.; Welter, R.; Malaman, B. *Nanostruct. Mater.* **1999**, *12*, 641−644.
(27) Ekwall, P.; Mandell, L.; Fontell, K. *J. Colloid Interface Sci.* **1970**, *33*, 215−235.